

# Dihydroartemisinin inhibits liver cancer cell migration and invasion by reducing ATP synthase production through CaMKK2/NCLX

JIANG CHANG<sup>1\*</sup>, CHENGYI XIN<sup>2\*</sup>, YONG WANG<sup>3</sup> and YING WANG<sup>4</sup>

<sup>1</sup>Department of Hepatopancreatobiliary Surgery, The First Affiliated Hospital of Hainan Medical University, Haikou, Hainan 570102; <sup>2</sup>Department of Pharmacy, Bayannur Hospital, Bayannur, Inner Mongolia Autonomous Region 015000; <sup>3</sup>Department of Neurosurgery, Hainan West Central Hospital, Danzhou, Hainan 571700; <sup>4</sup>Department of General Practice, The First Affiliated Hospital of Hainan Medical University, Haikou, Hainan 570102, P.R. China

Received May 20, 2023; Accepted September 8, 2023

DOI: 10.3892/ol.2023.14127

**Abstract.** Calcium/calmodulin-dependent protein kinase 2 (CaMKK2) and mitochondrial sodium/calcium exchanger protein (NCLX) are key regulatory factors in calcium homeostasis. Finding natural drugs that target regulators of calcium homeostasis is critical. Dihydroartemisinin (DHA) is considered to have anticancer effects. The present study aimed to investigate the mechanism of DHA in regulating liver cancer migration and invasion. The present study used HepG2 and HuH-7 cells and overexpressed CaMKK2 and knocked down CaMKK2 and NCLX. The antiproliferative activity of DHA on liver cancer cells was assessed through colony formation and EdU assays. Cell apoptosis was detected through YO-PRO-1/PI staining. The levels of reactive oxygen species (ROS) were measured using a ROS detection kit (DCFH-DA fluorescent probe). Cell migratory and invasive abilities were examined using wound healing and Transwell assays. The ATP production of liver cancer cells was detected using ATP fluorescent probes. Cell microfilaments were monitored for changes using Actin-Tracker Green-488. The effects of DHA on the expression of CaMKK2, NCLX, sodium/potassium-transporting ATPase subunit  $\alpha$ -1 (ATP1A1) and ATP synthase subunit d, mitochondrial (ATP5H) were determined by western blotting and reverse transcription-quantitative PCR. The results revealed that DHA significantly inhibited proliferation, reduced ROS levels and promoted apoptosis in liver

cancer cells. CaMKK2 overexpression significantly enhanced the invasive and migratory ability of liver cancer cells, whereas DHA inhibited the pro-migratory effects of CaMKK2 overexpression. DHA significantly reduced the mitochondrial ATP production and altered the arrangement of microfilaments in liver cancer cells. In addition, DHA significantly decreased the expression of CaMKK2, NCLX, ATP1A1 and ATP5H. Furthermore, by knockdown experiments of NCLX the results demonstrated that CaMKK2 downregulated the expression of ATP1A1 and ATP5H in liver cancer cells through NCLX. In conclusion, DHA may reduce ATP synthase production via the CaMKK2/NCLX signaling pathway to inhibit the invasive phenotype of liver cancer cells. It is essential to further investigate the effectiveness of DHA in the anticancer mechanism of liver cancer cells.

## Introduction

Calcium homeostasis-related proteins have been identified as crucial driving factors that regulate ATP synthesis and influence tumorigenesis and progression, and are closely associated with the proliferation, differentiation and metastasis of cancer cells (including cervical cancer) (1). Resveratrol specifically kills cancer cells by an increase in the  $\text{Ca}^{2+}$  coupling between the endoplasmic reticulum and mitochondria (2). Calcium/calmodulin-dependent protein kinase kinase 2 (CaMKK2) is a calcium-dependent protein kinase and its activation can promote glycolysis, mitochondrial respiration and fatty acid metabolism, which increases the viability of tumor cells (3). The regulation of CaMKK2 can vary with prostate cancer, and in a previous study CaMKK2 was reported to be a direct target of the androgen receptor in prostate cancer cells (4). CaMKK2 inhibitors can reduce the proliferation and metastatic ability of lung cancer cells *in vivo* (5). Targeting CaMKK2 expression can improve the survival rate of patients with liver cancer and inhibit the tumorigenicity of liver cancer cells in *in vivo* models (6). By mediating calmodulin activation, CaMKK2 promotes the accumulation of calcium ions in cancer cells to activate EGFR and decrease the survival of these cells (7). The mitochondrial sodium/calcium exchanger

*Correspondence to:* Dr Ying Wang, Department of General Practice, The First Affiliated Hospital of Hainan Medical University, 31 Longhua Road, Longhua, Haikou, Hainan 570102, P.R. China  
E-mail: wyl8876841575@126.com

\*Contributed equally

**Key words:** dihydroartemisinin, liver cancer, ATP synthase, calcium/calmodulin-dependent protein kinase 2, mitochondrial sodium/calcium exchanger protein, metastasis

protein (NCLX) is a sodium-calcium ion exchange protein involved in the proliferation, differentiation and metastasis of cancer cells by maintaining intracellular calcium ion balance (8). A previous study demonstrated that knocking down NCLX significantly reduced mitochondrial ATP generation and inhibited the proliferation and tumor growth of colorectal cancer cells (9). In human colorectal tumors and spontaneous colorectal cancer mouse models, downregulation of NCLX leads to mitochondrial calcium overload, mitochondrial depolarization, reduced expression of cell cycle genes and inhibition of the growth of the xenograft tumor (8). CGP37157, a benzodiazepine derivative, promotes mitochondrial damage and induces cell apoptosis by inhibiting NCLX expression in neuronal cells (10). CaMKK2 and NCLX both serve crucial roles in maintaining calcium homeostasis. However, the regulatory roles of CaMKK2 and NCLX in liver cancer cells are not clear.

The mechanism of energy metabolism regulation in liver cancer cells is complex, but ATP synthase is essential for energy metabolism (11,12). The expression level of ATP synthase is a key indicator reflecting the energy metabolism state of liver cancer cells (13). ATP synthase (ATP1A1 and ATP5H subunits) is involved in cell proliferation, division and the metastasis of liver cancer cells (13,14). High expression levels of ATP synthase subunit d, mitochondrial (ATP5H) are linked to poor prognosis of patients with ovarian cancer and are involved in cisplatin resistance, cell experiments have shown that dihydroartemisinin (DHA) treatment can reduce the side effects of cisplatin and reverse cisplatin resistance (15). Nevertheless, elevated NRF2 may mediate DHA resistance in head and neck squamous cell carcinoma (16). Epigenetic loss of the ATP synthase subunit ATP5H triggers a core metabolic reprogramming pathway, leading to reactive oxygen species (ROS) accumulation and elevated hypoxia induced factor-1 $\alpha$ , thereby promoting multiple drug resistance in tumor cells (17). Bufalin inhibits tumorigenesis in liver cancer cells by regulating sodium/potassium-transporting ATPase subunit  $\alpha$ -1 (ATP1A1)/carbonic anhydrase 2 signaling (18). ATP1A1 has been associated with the tamoxifen resistance of breast cancer through screening of super-enhancer-associated proteins (19). Homologous ATP1A1 binding between ATP1A1-overexpressing tumor cells and fibroblasts was found in pancreatic ductal adenocarcinoma cells (20). Activin A secreted by fibroblasts induces EMT of tumor cells and activation of myofibroblasts (20). Disrupting ion homeostasis in cancer cells can synergize with MAPK pathway inhibitors to promote melanoma regression *in vivo* (21).

DHA, a derivative of artemisinin, has shown potential antitumor effects in cancer therapy (22). DHA can induce ferroptosis of cervical cancer cells by regulating the production of ROS and accumulation of malondialdehyde, and when paired with doxorubicin, DHA can inhibit the proliferation and metastasis of cervical cancer cells (23). DHA can reduce the proliferation of breast cancer cells by inhibiting STAT3 phosphorylation, inducing apoptosis and reversing cisplatin resistance (24). DHA exerts antitumor effects by inhibiting glycolysis, promoting autophagy and inducing mitochondrial ATP production (25). The present study investigated the effects of DHA on the mitochondrial function, cytoskeleton, proliferation, migration and invasion of liver cancer cells

through ATP probes, ROS, cytoskeleton, colony formation, EDU, cell scratch, and Transwell experiments. By constructing CaMKK2 and NCLX siRNA cell models, it investigated whether DHA inhibited cancer cell proliferation, reduced ATP and ROS production, promoted cytoskeletal recombination and inhibited the invasive phenotype of cancer cells through the CaMKK2/NCLX axis.

## Materials and methods

**Cell culture and transfection.** Human liver cancer cells HepG2 and HuH-7 were purchased from the Cell Bank of Type Culture Collection of The Chinese Academy of Sciences and were grown in Dulbecco's Modified Eagle Medium (DMEM; Gibco; Thermo Fisher Scientific, Inc.) with 10% fetal bovine serum (FBS; Gibco; Thermo Fisher Scientific, Inc.) and 1% penicillin/streptomycin (Gibco; Thermo Fisher Scientific, Inc.) at 37°C with 5% CO<sub>2</sub>. Short tandem repeat profiling was used to verify the HepG2 and HuH-7 cell lines. DHA was purchased from MedChemExpress (cat. no. HY-N0176; purity,  $\geq 99.0\%$ ) and was dissolved in DMSO with the final working concentration as 10  $\mu$ M at room temperature (19) and DMSO was used as a control. Full-length CaMKK2 (Sangon Biotech Co., Ltd.) was cloned into the pcDNA3.1(+)-ZB02427 vector (Sangon Biotech Co., Ltd.). Sangon Biotech was the supplier of CaMKK2 and the plasmid backbone. A total of 2.5  $\mu$ g CaMKK2 overexpression (OE) plasmid was used for transfection. Then transfection with Lipo8000 (cat. no. C0533; Beyotime Institute of Biotechnology) at 37°C for 24 h. Empty vector was utilized as a negative control (NC). Small interfering (si)RNAs were purchased from Sangon Biotech Co., Ltd., and their sequences were as follows: NCLX siRNA1 (sense, 5'-UGAGUGUGCUUUGUGUGCUGCUAAU-3', and antisense 5'-AUUAGCAGCACACAAAGCACACUCA-3'), NCLX siRNA2 (sense, 5'-GGGAAUGGUGCACCUGAC AUCUUCA-3', and antisense, 5'-UGAAGAUGUCAGGUG CACCAUUCUU-3'), NCLX siRNA3 (sense, 5'-CCGGGUAUC UUCUAAUACCAATT-3' and antisense, 5'-UUGGUAUUA GAAGAUACCCGGTT-3'), CaMKK2 siRNA1 (sense, 5'-GAU GAAAUUGGAAAGGGCUCCUAUG-3' and antisense, 5'-CAUAGGAGCCCUUCCAAUUAUUAUC-3') CaMKK2 siRNA2 (sense, 5'-CCCAUUGAGCAGGUGUACCAGGAA A-3', and antisense, 5'-UUUCCUGGUACACCUGCUCAA UGGG-3') CaMKK2 siRNA3 (sense, 5'-CAAUACCUACUA UGCAUGAATT-3' and antisense, 5'-UUCAUUGCAUAG UAGGUAUUGTT-3') and siRNA-NC (sense, 5'-UUCUCC GAACGUGUCACGUTT-3' and antisense, 5'-ACGUGACAC GUUCGGAGAATT-3'). For all plasmid and siRNA Sequence transfections, HepG2 and HuH-7 cells were seeded in 6-well plates (2x10<sup>5</sup> cells/well) and incubated at 37°C and 5% CO<sub>2</sub> for 24 h. Then, 100 pmol siRNA was added per well and Lipo8000 (cat. no. C0533; Beyotime Institute of Biotechnology) used for transfection at room temperature for 24 h. Cells were collected for subsequent western blotting assays to confirm the success of the transfections. After successful transfection the cells were incubated at 37°C and 5% CO<sub>2</sub> for 24 h prior to subsequent experiments.

**EdU-594 staining.** The BeyoClick™ EdU-594 cell proliferation assay kit with Alexa Flour 594 (cat. no. C0078S; Beyotime

Institute of Biotechnology) was used according to the manufacturer's instructions. HepG2 and HuH-7 cells ( $4 \times 10^4$  cells/well) were seeded in 96-well plates and incubated at 37°C in a 5% CO<sub>2</sub> atmosphere. The cells were treated with 10  $\mu$ M EDU solution for 2 h at 37°C. Then, Click reaction solution was added and the cells were incubated for 30 min at room temperature, then washed three times with PBS. Cells were stained with DAPI (10  $\mu$ g/ml) for 10 min at room temperature, and were subsequently imaged using a fluorescence microscope (Leica Microsystems GmbH). Data were analyzed by Image-Pro Plus Software 6.0 (Media Cybernetics, Inc.).

**Transwell migration assay.** HepG2 and HuH-7 cells were starved without serum for 24 h in 6-well plates at 37°C. Cells were collected, resuspended in 200  $\mu$ l serum-free DMEM to  $1 \times 10^5$  cells/ml and added to 24-well upper chambers (Corning, Inc.). A total of 600  $\mu$ l DMEM with 10% FBS was added to the lower chambers. After incubating for 48 h at 37°C, cells were fixed with 4% paraformaldehyde for 10 min at room temperature and stained using 0.1% crystal violet for 20 min at room temperature. Cells that did not pass through the Transwell membrane were wiped away with a cotton swab following the staining. Matrigel inserts were used (coated in the chambers at 37°C for 5 h); the subsequent steps were identical to the migration assay. The remaining cells were imaged using a light microscope (Olympus Corporation). The invaded cells were counted via Image-Pro Plus Software 6.0 (Media Cybernetics, USA).

**Wound healing assay.** HepG2 and HuH-7 cells were seeded in 6-well plates ( $5 \times 10^5$  cells/well) and cultured at 37°C with 5% CO<sub>2</sub> until cell confluence was >90%. A single scratch was made in the cell monolayer using a 200  $\mu$ l pipette tip. After washing with PBS three times, DMEM with 1% FBS was added to each well (26) and cells were imaged at 0 and 48 h using a light microscope. The migration rate was calculated using the following formula: Migration rate (%) =  $(S_0 - S_{48\text{ h}}) / S_0 \times 100$ .  $S_0$  h represents the distance of the scratch at 0 and  $S_{48\text{ h}}$  represents the distance at 48 h (27). Wound healing was analyzed using the Image-Pro Plus Software 6.0 (Media Cybernetics, USA).

**Colony formation assay.** HepG2 and HuH-7 cells were seeded in 3.5 cm plates at ~200 cells/well in DMEM with 10% FBS. The groups treated with CaMKK2-OE, NCLX knockout and DHA were incubated at 37°C for 24 h. Then, the treated cells were cultured for ~15 days until visible colonies (>50 cells) formed. The supernatant was discarded and cells were washed twice with PBS. Subsequently, cells were fixed with 4% paraformaldehyde for 15 min at room temperature, stained with 0.1% crystal violet for 20 min at room temperature, washed twice with PBS and air-dried. A light microscope (Olympus Corporation) was used to image cells and the colonies counted manually.

**Western blotting.** HepG2 and HuH-7 cells were lysed with RIPA lysis buffer (Nanjing KeyGen Biotech Co., Ltd.) on ice for 25 min. Total cellular protein concentration was determined using a BCA protein assay kit (Leagene Biotechnology). SDS-PAGE loading buffer (5X; Beijing Zoman Biotechnology

Co., Ltd.) was used to denature the proteins at 100°C for 10 min. 30 ng proteins were then separated by 9% SDS-PAGE and transferred onto PVDF membranes. The PVDF membranes were incubated with 5% skimmed milk dissolved in TBS-1% Tween 20 (TBST) at room temperature for 1 h. After blocking, membranes were incubated with primary antibodies overnight at 4°C. The primary antibodies and corresponding dilutions used were as follows: Anti-ATP1A1 (1:5,000; cat. no. 14418-1-AP; Wuhan Sanying Biotechnology), anti-ATP5H (1:500; cat. no. 17589-1-AP; Wuhan Sanying Biotechnology), anti-NCLX (1:1,000; cat. no. 21430-1-AP; Wuhan Sanying Biotechnology), anti-CaMKK2 (1:500; cat. no. 11549-1-AP; Wuhan Sanying Biotechnology) and anti- $\beta$ -actin (1:2,000; cat. no. 20536-1-AP; Wuhan Sanying Biotechnology). The membranes were then washed with TBST three times and incubated with anti-rabbit horse-radish peroxidase-conjugated secondary antibodies (1:5,000; cat. no. ZB-2301; OriGene Technologies, Inc.) at room temperature for 1 h. The membranes were visualized using an ECL kit (cat. no. A38554; Thermo Fisher Scientific, Inc.) and analyzed with Image-Pro Plus Software 6.0 (Media Cybernetics, Inc.).

**Intracellular detection of ROS levels.** ROS levels were detected using ROS Assay Kit (cat. no. S0033, Beyotime Institute of Biotechnology) according to manufacturer's instructions. Briefly, HepG2 and HuH-7 cells were seeded in 6-well plates ( $1 \times 10^5$  cells/well) and incubated with 2',7'-dichlorofluorescein diacetate (10  $\mu$ M) at 37°C for 20 min. A fluorescence microscope was then used to image cells. The level of intracellular ROS was expressed as the fluorescence intensity. Data analysis were performed using Image-Pro Plus Software 6.0 (Media Cybernetics, Inc.).

**Detection of apoptosis by YO-PRO-1/PI staining.** The Apoptosis and Necrosis Detection Kit with YO-PRO-1 and PI (cat. no. C1075; Beyotime Institute of Biotechnology) was used according to the manufacturer's instructions. YO-PRO-1/PI working solution was added to HepG2 and HuH-7 cells ( $5 \times 10^5$  cells/well) were seeded in a 6-well plate, then cells were incubated at 37°C for 20 min in the dark. After incubation, cells were imaged using a fluorescence microscope. Apoptotic and necrotic cells exhibited green and red fluorescence, with overlapping orange yellow fluorescence. The percentage of apoptotic and necrotic cells was manually counted and calculated.

**Reverse transcription-quantitative PCR (RT-qPCR).** TRIzol® (Thermo Fisher Scientific, Inc.) was used for RNA extraction from HepG2 and HuH-7 cells. cDNA was synthesized using the RevertAid First Strand cDNA Synthesis Kit (Thermo Fisher Scientific, Inc.) according to the manufacturer's instructions. qPCR was performed according to the instructions of PowerUp™ SYBR™ Green Master Mix (Applied Biosystems; Thermo Fisher Scientific, Inc.). Thermocycling consisted of 20 sec of initial denaturation at 95°C, followed by 35 cycles with 20 sec at 95°C for denaturation and 20 sec at 60°C for annealing and extension. Gene-specific primers were synthesized by Sangon Biotech Co., Ltd. The primer sequences used were as follows: ATP1A1 forward (F), 5'-TGCCCTGGAATGGGTGTTGCT-3' and reverse (R), 5'-TTCTCCACCAGCCGCCAGG-3'; ATP5H F, 5'-TAATGCGCTGAAGGT

TCCCG-3' and R, 5'-GAGAGACACCCACTCAGCAC-3'; CaMKK2 F, 5'-ATGGGCACATCAAGATCGCT-3' and R, 5'-CATCCAAGGCCTTCCCAGAG-3'; NCLX F, 5'-GCC TTCTCTGACCCGCACAC-3' and R, 5'-CCTCTCCGTTGC CGTTGGTAG-3'; and GAPDH F, 5'-TCAAGATCATCAGCA ATGCC-3' and R, 5'-CGATACCAAAGTTGTTCATGGA-3'. Relative gene expression levels were normalized using the  $2^{-\Delta\Delta C_q}$  method (28). GAPDH was used as the reference gene.

**F-actin microfilament staining.** Imaging of the microfilaments of HepG2 and HuH-7 cells was carried out according to the instruction of Actin-Tracker Green-488 (Beyotime Institute of Biotechnology). HepG2 and HuH-7 cells ( $5 \times 10^5$  cells/well) were seeded in a 6-well plate. They were fixed with 3.7% formaldehyde in PBS at room temperature for 20 min. Then, the cells were incubated with Actin-Tracker Green-488 solution labeled with phalloidin in the dark for 30 min and observed with a fluorescence microscope. Finally, DAPI (10  $\mu$ g/ml) staining solution was used to re-stain the nuclei for 5 min at room temperature. All staining was quantified using Image-Pro Plus Software 6.0 (Media Cybernetics, Inc.). Phalloidin-stained areas were expressed as percentage of whole areas per microscopic field (29). The fluorescence intensities were measured with Image-Pro Plus Software 6.0 (Media Cybernetics, Inc.).

**Detection of ATP content.** ATP fluorescent probe (pCMV-AT1.03) was purchased from (Beyotime Institute of Biotechnology). pCMV-AT1.03 is a plasmid tool used to express AT1.031 protein as an ATP fluorescence probe in cells. Following transfection, the AT1.031 protein is primarily found in the cytoplasm where it can detect changes in ATP content and produce fluorescence when it binds to ATP. HepG2 and HuH-7 cells ( $2 \times 10^5$  cells/well) were seeded into 12-well plates and cultured at 37° with 5% CO<sub>2</sub> for 24 h. Subsequently, 1  $\mu$ g of ATP fluorescent probe was added per well and Lipo8000 (cat. no. C0533; Beyotime Institute of Biotechnology) used for transfection for 24 h at 37°C. After cells were transfected with CaMKK2-OE and NCLX siRNA and/or DHA for 24 h at 37°C, cells were imaged using a fluorescence microscope. The image was analyzed with Image-Pro Plus Software 6.0 (Media Cybernetics, USA).

**Statistical analysis.** SPSS software (version 17.0; SPSS, Inc.) was used for data analysis, and the data are presented as the mean  $\pm$  standard deviation. Differences between groups were compared with one-way analysis of variance followed by Bonferroni post hoc test. Data were visualized using GraphPad Prism software (version 8.0; Dotmatics).  $P < 0.05$  was considered to indicate a statistically significant difference.

## Results

**Effects of DHA treatment, CaMKK2-OE and NCLX knockdown on the proliferation and apoptosis of liver cancer cells.** NCLX and CaMKK2 siRNA-mediated knockdown and CaMKK2-OE in HepG2 and HuH-7 cells were verified through western blotting (Fig. 1). The transfection effect of NCLX siRNA3 was more significant, so this was chosen for the following experiments (Fig. 1A-D). The overexpression of CaMKK2 was significant (Fig. 1E-H). The transfection effect

of CaMKK2 siRNA3 was more significant, which was chosen for follow-up experiments (Fig. 1I-L).

Colony formation assay and EdU staining were used to analyze the proliferation rate of these cells. These assays demonstrated that CaMKK2-OE significantly increased cell proliferation compared with the OE-NC group. DHA treatment and NCLX knockdown significantly inhibited proliferation compared with CaMKK2-OE group (Figs. 2A-D and S1). In addition, analysis of apoptosis and necrosis demonstrated that following DHA treatment or NCLX knockdown in CaMKK2-OE group significantly increased the number of apoptotic and necrotic liver cancer cells (Fig. 2E-G). NCLX siRNA alone and DHA alone also significantly inhibited proliferation and increased the number of apoptosis and necrosis of cancer cells.

**Effects of DHA treatment, CaMKK2-OE and NCLX knockdown on liver cancer cell migration and invasion.** Transwell assays were used to detect the invasive capacity of liver cancer cells. The number of invasive cells increased significantly in the CaMKK2-OE group compared with OE-NC (Fig. 3A-D). DHA treatment and NCLX knockdown in CaMKK2-OE cells significantly reduced the number of invasive cells compared with the CaMKK2-OE group. Additionally NCLX siRNA alone also reduced the number of migration and invasion cells.

The migratory ability of liver cancer cells was detected via wound healing assays. These assays demonstrated that CaMKK2-OE significantly increased the migration of liver cancer cells compared with OE-NC (Fig. 4A-D). After DHA treatment and NCLX knockdown in CaMKK2-OE cells, the wound healing rate of the cells was significantly decreased and the migrating distance was reduced compared with the CaMKK2-OE group. Although CaMKK2-OE promoted the migration and invasion of liver cancer cells, this effect could be inhibited by DHA treatment and NCLX siRNA. Therefore, NCLX may be a critical regulator in CaMKK2-mediated liver cancer cell metastasis and CaMKK2 may be an effective target of DHA.

**Effects of different treatments on the formation of ATP and ROS in liver cancer cells.** The effects of different treatment groups on the production of ATP and ROS in cancer cells after 24 h of intervention were analyzed. The results of ATP fluorescence probe experiments showed that the fluorescence intensity of CaMKK2-OE group was significantly increased compared with OE-NC, while DHA treatment or NCLX knockout resulted in a significant decrease in CaMKK2-OE group (Fig. 5A-D). In the CaMKK2-OE group, intracellular ROS levels were significantly higher compared with the OE-NC group (Fig. 5E-H). However, after DHA treatment or NCLX knockout, the ROS level in the CaMKK2-OE treatment group was significantly reduced. Therefore, DHA treatment and NCLX siRNA reduced the production of ATP and ROS, indicating that DHA may play an anti-cancer role by reducing the energy metabolism of cancer cells. In addition, it was also demonstrated that NCLX siRNA could block CaMKK2-regulated ATP and ROS production.

**Liver cancer cell cytoskeletal remodeling.** Changes in cancer cell microfilaments were observed in the CaMKK2-OE



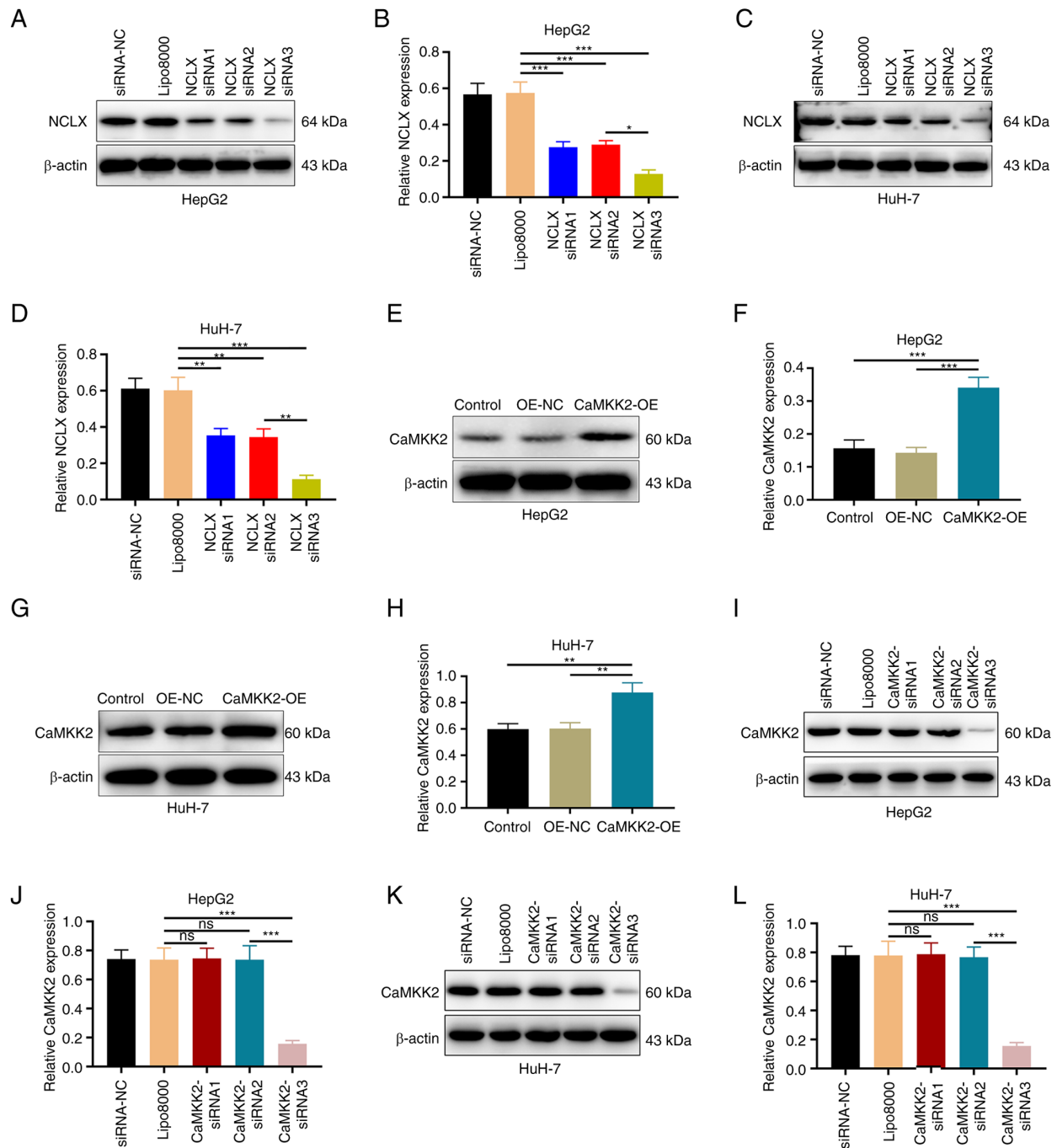


Figure 1. Protein expression levels of NCLX and CaMKK2 in HepG2 and HuH-7 cells. Protein expression levels of NCLX in (A and B) HepG2 and (C and D) HuH-7 cells transfected with NCLX siRNA. Protein expression levels of CaMKK2 of (E and F) HepG2 cells and (G and H) HuH-7 cells transfected with CaMKK2-OE plasmid. Protein expression levels of CaMKK2 in (I and J) HepG2 and (K and L) HuH-7 cells transfected with CaMKK2 siRNA. All data are presented as the mean  $\pm$  standard deviation (n=3). Data were analyzed using one-way analysis of variance followed by Bonferroni post hoc test. \*\*P<0.01; \*\*\*P<0.001. NCLX, mitochondrial sodium/calcium exchanger protein; CaMKK2, calcium/calmodulin-dependent protein kinase kinase 2; siRNA, small interfering RNA; OE, overexpression; NC, negative control; ns, not significant.

group. Compared with the OE-NC group, the fluorescence intensity of the microfilaments in the CaMKK2-OE group was significantly enhanced, and the microfilaments were increased and stretched. However, knockdown of NCLX or DHA treatment significantly reduced the fluorescence intensity of microfilaments, resulting in microfilament shortening and decomposition. Similar results were obtained after knock-down of NCLX or DHA treatment in the CaMKK2-OE group (Fig. 6A-D).

*Effects of DHA treatment, CaMKK2-OE and NCLX knock-down on ATP synthase expression in liver cancer cells.* The present study showed that compared with the OE-NC group, the mRNA and protein expression levels of CaMKK2, NCLX, ATP1A1 and ATP5H were upregulated in the CaMKK2 OE group. Compared with the CaMKK2-OE group, DHA treatment reduced the expression levels of CaMKK2, NCLX, ATP1A1 and ATP5H, and reversed the effect of CaMKK2-OE induction (Figs. 7A-H and 8A-J). After knocking down NCLX

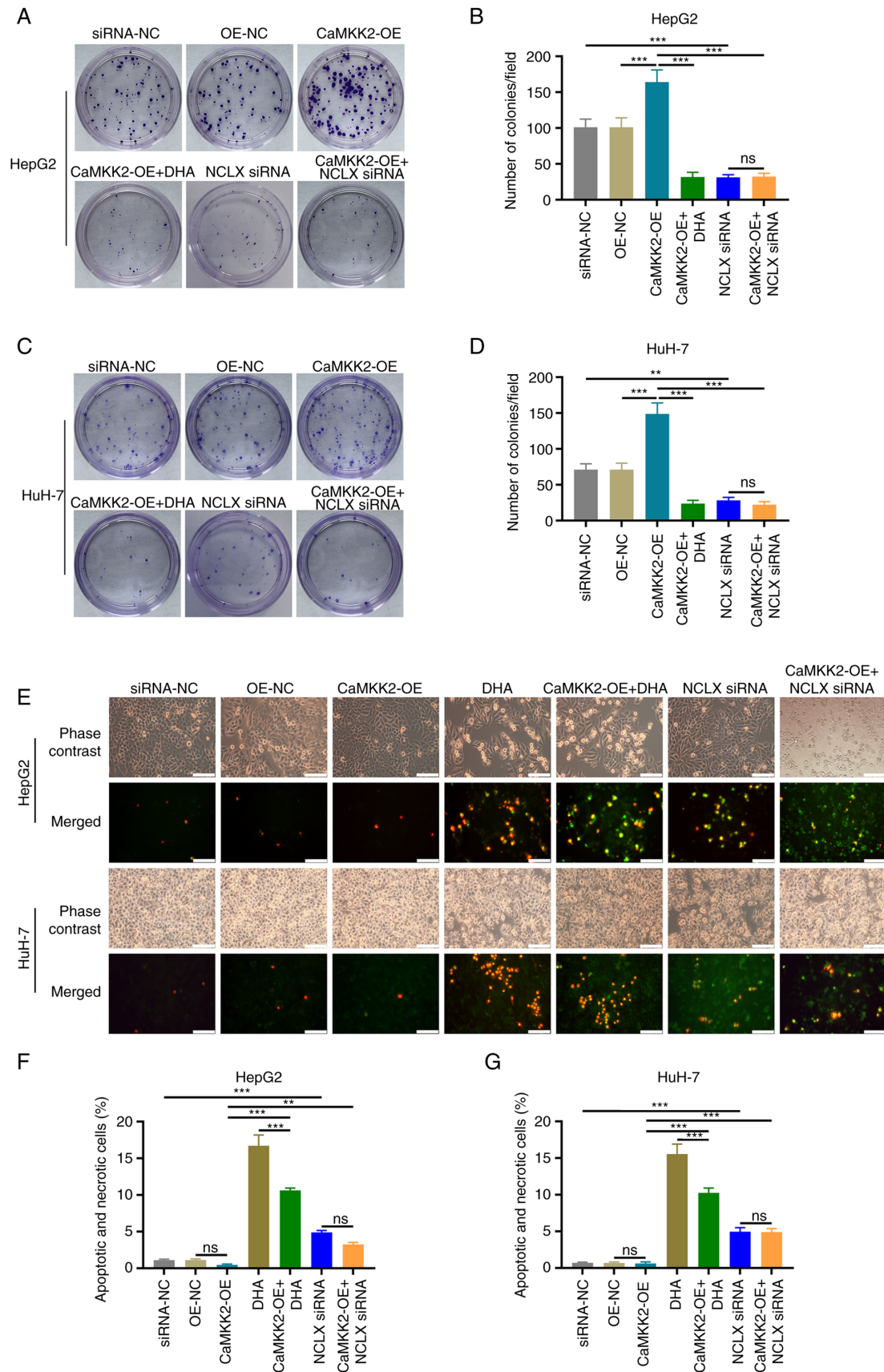


Figure 2. Effects of DHA, CaMKK2 and NCLX on the proliferation and apoptosis of liver cancer cells. (A) Colony formation assay and (B) number of HepG2 colonies formed with cells treated with DHA, CaMKK2-OE and NCLX siRNA. (C) Colony formation assay and (D) number of HuH-7 colonies formed with cells treated with DHA, CaMKK2-OE and NCLX siRNA. Transfected (E) HepG2 and HuH-7 cells stained with YO-PRO-1 and PI dye and treated with DHA, CaMKK2-OE and NCLX siRNA. Apoptosis and necrosis rate of (F) HepG2 and (G) HuH-7 cells treated with DHA, CaMKK2-OE and NCLX siRNA. All data are presented as the mean  $\pm$  standard deviation (n=3). Data were analyzed using one-way analysis of variance followed by Bonferroni post hoc test. Scale bar, 50  $\mu$ m \*\*\*P<0.01; \*\*P<0.001. ns, not significant; NCLX, mitochondrial sodium/calcium exchanger protein; DHA, dihydroartemisinin; CaMKK2, calcium/calmodulin-dependent protein kinase kinase 2; siRNA, small interfering RNA; OE, overexpression; NC, negative control.

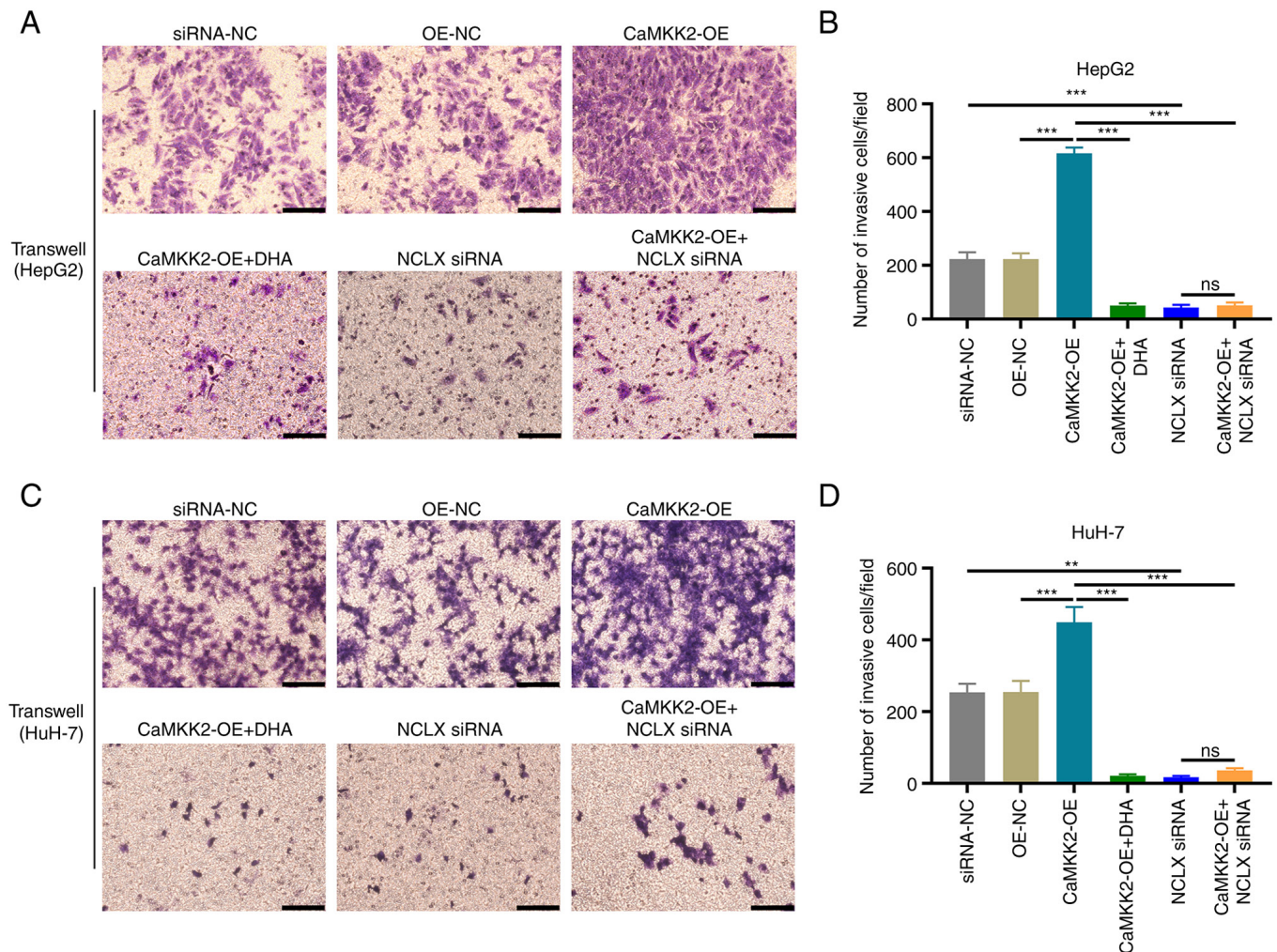


Figure 3. Effect of DHA treatment, CaMKK2-OE and NCLX siRNA on the invasive capacity of liver cancer cells. (A) Transwell assay of HepG2 cells treated with DHA, CaMKK2-OE and/or NCLX siRNA and (B) number of invasive cells per field. (C) Transwell assay of HuH-7 cells treated with DHA, CaMKK2-OE and/or NCLX siRNA and (D) number of invasive cells per field. Scale bar, 50  $\mu$ m. All data are presented as the mean  $\pm$  standard deviation (n=3). Data were analyzed using one-way analysis of variance followed by Bonferroni post hoc test. \*\*P<0.01; \*\*\*P<0.001. NCLX, mitochondrial sodium/calcium exchanger protein; DHA, dihydroartemisinin; CaMKK2, calcium/calmodulin-dependent protein kinase kinase 2; siRNA, small interfering RNA; OE, overexpression; ns, not significant; NC, negative control.

in CaMKK2 OE group, the expression level of CaMKK2 protein was significantly increased compared with OE-NC, while NCLX, ATP1A1 and ATP5H expression significantly decreased (Fig. 9A-J). The above results showed that knock-down of NCLX had no effect on the expression of CaMKK2. On the contrary, knockdown of CaMKK2 significantly reduced the expression of NCLX, ATP1A1 and ATP5H. Therefore, NCLX may be a downstream gene of CaMKK2, which mediates the regulation of CaMKK2-induced ATP synthase (ATP1A1 and ATP5H subunits) in the energy metabolism pathway. Based on the above experimental results, DHA can target the CaMKK2/NCLX gene, inhibit the production of ATP synthase and destroy the energy metabolism pathway and thus may play an anti-cancer role.

## Discussion

Targeting energy metabolism pathways in tumors is an effective strategy for inhibiting metastasis (30). Energy metabolism pathways in cancer cells serve a crucial role in

sustaining their biological behavior and promoting metastasis (31). Mitochondrial calcium-regulating proteins affect cellular energy metabolism by activating oxidative metabolism, mitochondrial respiration and ATP synthesis (32,33). CaMKK2 and NCLX serve important roles in physiological or pathological processes, such as maintaining cellular energy homeostasis and cell proliferation (34,35). In the study of gastric cancer, the application of small molecule inhibitors of calcium-regulated protein can significantly inhibit the peritoneal metastasis of gastric cancer cells (36). The drugs that regulate the release of calcium ions have synergistic anti-proliferative effects in combination with gemcitabine, oxaliplatin and adriamycin (37). Therefore, the development of drugs targeting calcium-regulating proteins has become a focus of cancer treatment (38). DHA is considered an efficient anticancer agent, but its molecular mechanism of action is not clear (24). DHA can inhibit the proliferation activity of glioma U87 and U251 cells, increase ROS level and promote apoptosis (39). The present study demonstrated that DHA can significantly inhibit the expression of CaMKK2 and



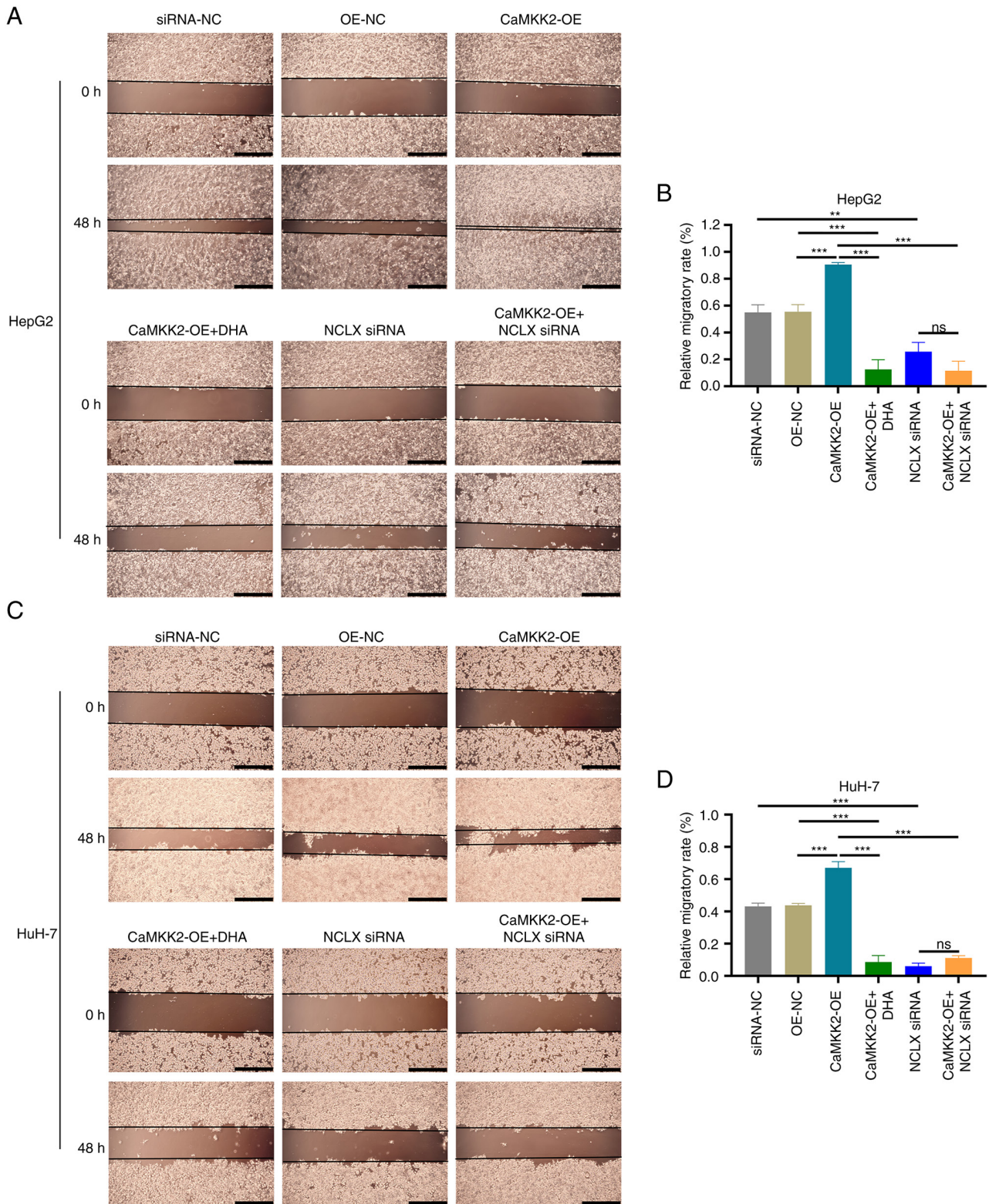


Figure 4. Effects of DHA treatment, CaMKK2-OE and NCLX siRNA on the migratory capacity of liver cancer cells. (A) Wound healing assay of HepG2 cells treated with DHA, CaMKK2-OE and/or NCLX siRNA and (B) migrated distance after 48 h. (C) Wound healing assay of HuH-7 cells treated with DHA, CaMKK2-OE and/or NCLX siRNA and (D) migrated distance after 48 h. Scale bar, 200  $\mu$ m. All data are presented as the mean  $\pm$  standard deviation (n=3). Data were analyzed using one-way analysis of variance followed by Bonferroni post hoc test. \*\*P<0.01; \*\*\*P<0.001. NCLX, mitochondrial sodium/calcium exchanger protein; DHA, dihydroartemisinin; CaMKK2, calcium/calmodulin-dependent protein kinase 2; siRNA, small interfering RNA; ns, not significant; NC, negative control.

NCLX, suppress the proliferative activity of liver cancer cells, reduce the activity of ATP synthase, restructure the cytoskeleton and inhibit the migration and invasion of liver

cancer cells. Therefore, the present study demonstrated that the anticancer mechanism of DHA is mediated by the CaMKK2/NCLX signaling pathway, thereby inhibiting ATP

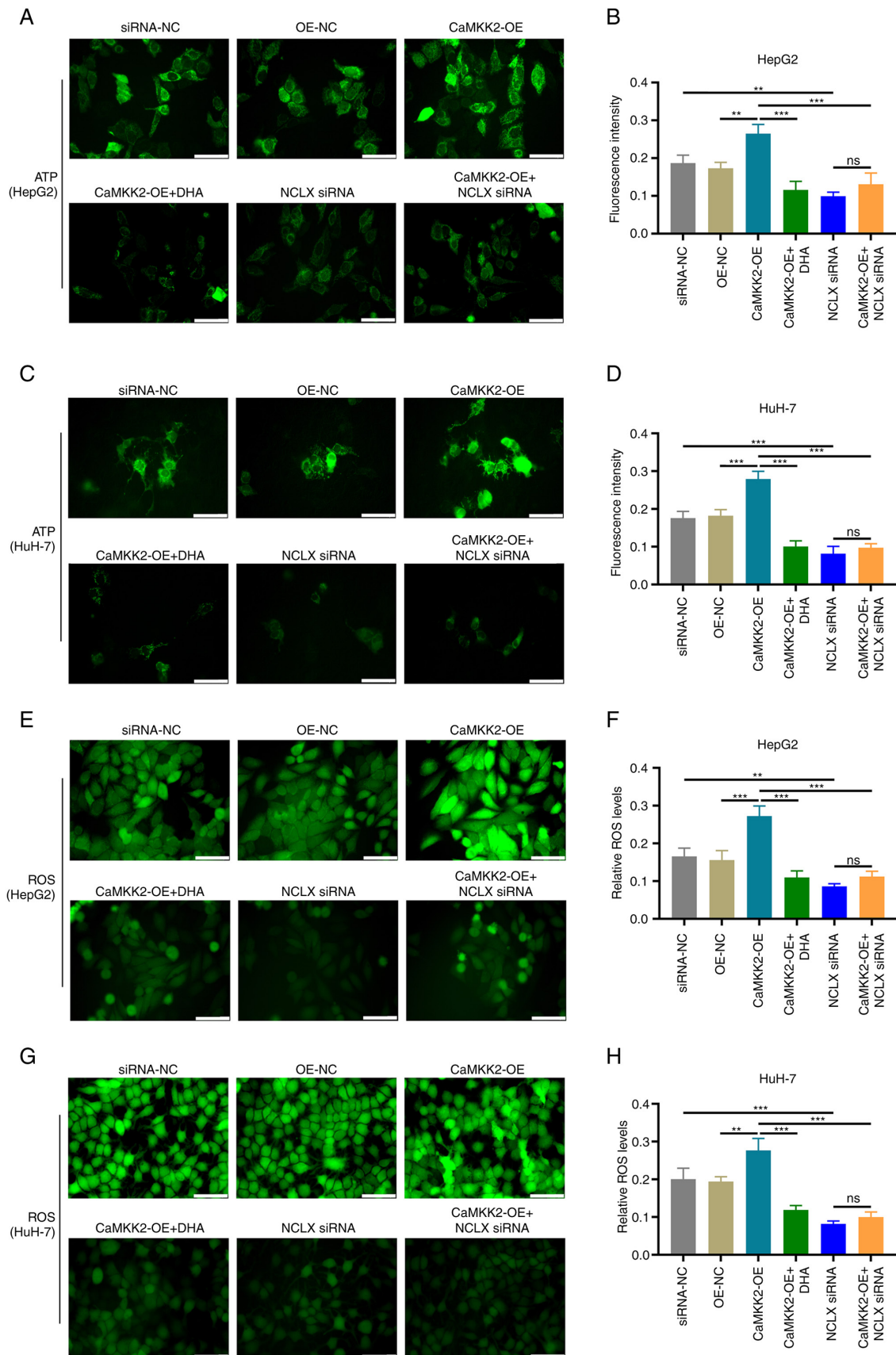


Figure 5. Effects of DHA treatment, CaMKK2-OE and NCLX siRNA on the production of ATP and ROS in liver cancer cells. (A) ATP levels and (B) fluorescence intensity of HepG2 cells treated with DHA, CaMKK2-OE and/or NCLX siRNA. (C) ATP levels and (D) fluorescence intensity of HuH-7 cells treated with DHA, CaMKK2-OE and/or NCLX siRNA. (E) Intracellular ROS levels and (F) fluorescence intensity of HepG2 cells treated with DHA, CaMKK2-OE and/or NCLX siRNA. (G) Intracellular ROS levels and (H) fluorescence intensity of HuH-7 cells treated with DHA, CaMKK2-OE and/or NCLX siRNA. Scale bar, 20  $\mu$ m. All data are presented as the mean  $\pm$  standard deviation (n=3). Data were analyzed using one-way analysis of variance followed by Bonferroni post hoc test. \*\*P<0.01; \*\*\*P<0.001. NCLX, mitochondrial sodium/calcium exchanger protein; DHA, dihydroartemisinin; CaMKK2, calcium/calmodulin-dependent protein kinase kinase 2; siRNA, small interfering RNA; OE, overexpression; ns, not significant; NC, negative control; ROS, reactive oxygen species.



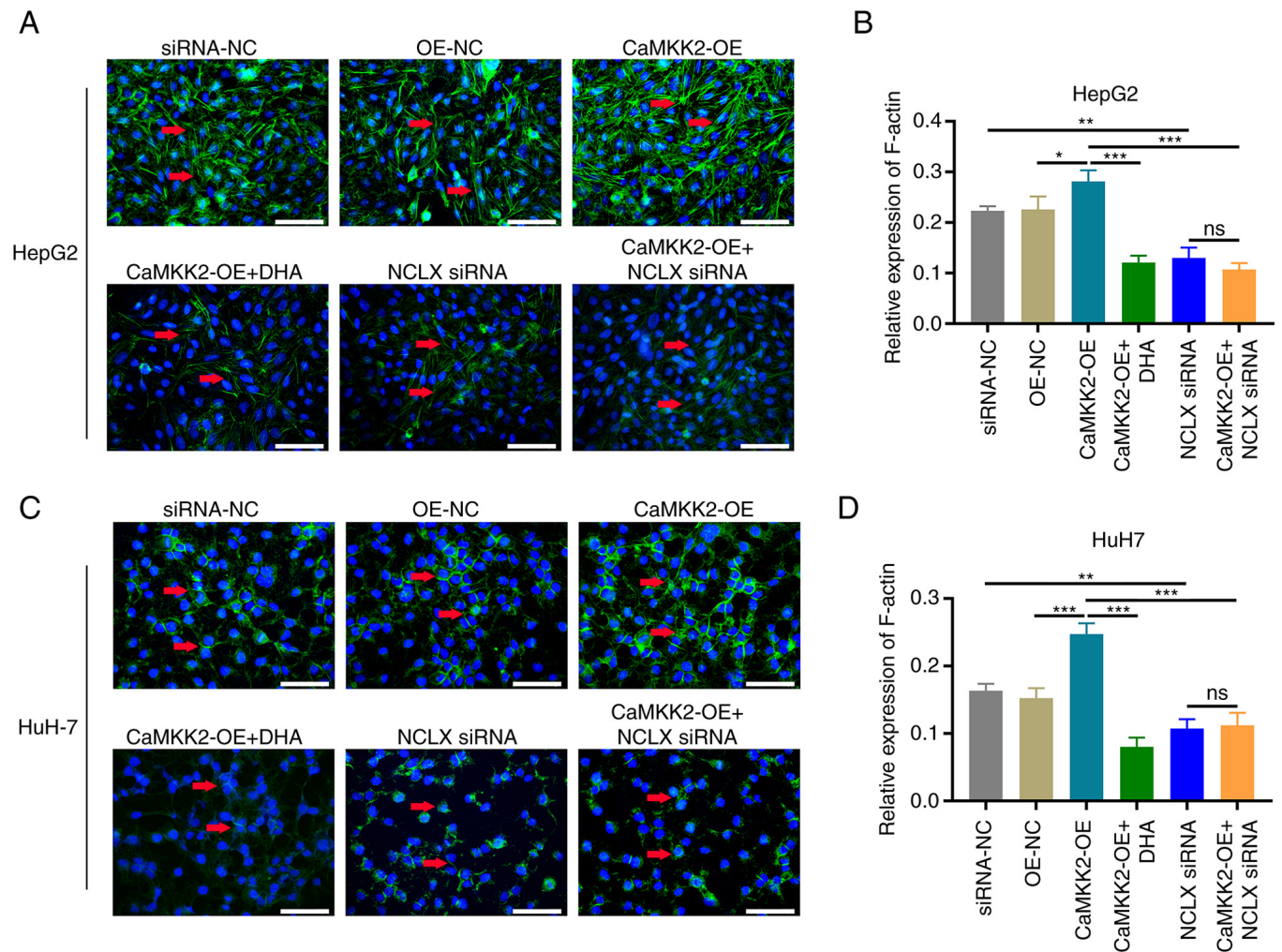


Figure 6. Effects of DHA treatment, CaMKK2-OE and NCLX siRNA on the actin cytoskeleton. (A) Phalloidin staining and (B) relative expression of F-actin in HepG2 cells treated with DHA, CaMKK2-OE and/or NCLX siRNA. (C) Phalloidin staining and (D) relative expression of F-actin in HuH-7 cells treated with DHA, CaMKK2-OE and/or NCLX siRNA. All data are presented as the mean  $\pm$  standard deviation ( $n=3$ ). Data were analyzed using one-way analysis of variance followed by Bonferroni post hoc test. Scale bar, 20  $\mu\text{m}$  \* $P<0.05$ ; \*\* $P<0.01$ ; \*\*\* $P<0.001$ . NCLX, mitochondrial sodium/calcium exchanger protein; DHA, dihydroartemisinin; CaMKK2, calcium/calmodulin-dependent protein kinase kinase 2; OE, overexpression; ns, not significant; NC, negative control.

synthase expression, which aims to provide a potential novel future treatment for liver cancer.

Mitochondrial calcium regulatory proteins are critical factors that determine cell function, shape and survival (40). In both cancer and non-cancer research, CaMKK2 has been reported to serve a key role in cell proliferation, and particularly in cancer cells it promotes cell proliferation, migration and invasion (41). CaMKK2 is overexpressed in various types of cancer, including prostate, breast, liver, ovarian and gastric cancers, contributing to their progression (41,42). In liver cancer, CaMKK2 expression is significantly upregulated and negatively correlated with the survival of patients with liver cancer (6). Knocking down CaMKK2 significantly inhibits proliferation of liver cancer cells and tumorigenicity in mouse models (6). Similarly, elevated levels of CaMKK2 have been implicated in promoting metastasis of gastric cancer cells, while downregulation of CaMKK2 significantly reduces cell proliferation and decreases gastric cancer cell migration and invasion (43). CaMKK2 serves as a valuable clinical biomarker and has the potential to be used as a therapeutic target for advanced prostate cancer (4). Furthermore,

CaMKK2 promotes tumor development by regulating cellular and systemic metabolism (1). In the present study, it was demonstrated that CaMKK2-OE significantly increased proliferation and colony formation in liver cancer cells, as well as promoting migration and invasion. These results are consistent with previously reported experimental results in gastric cancer cells (44). However, the present study further demonstrated that DHA significantly inhibited the effects induced by CaMKK2-OE. Therefore, CaMKK2 may be a target of the anticancer effect of DHA.

ATP is produced in mitochondria, which are the center of cellular energy metabolism. The  $\text{Ca}^{2+}$  overload in the mitochondrial matrix can induce an increase in ROS generation, trigger mitochondrial permeability transition pore opening and cytochrome *c* release and lead to cell apoptosis (45). DHA regulates ROS levels in liver cancer cells via multiple mechanisms (46). For example, DHA can increase the activity of antioxidant enzymes, such as superoxide dismutase and glutathione peroxidase, in liver cancer cells, thereby reducing ROS generation (47). DHA can also inhibit the activity of NADPH oxidase, thereby reducing the production of ROS (48).

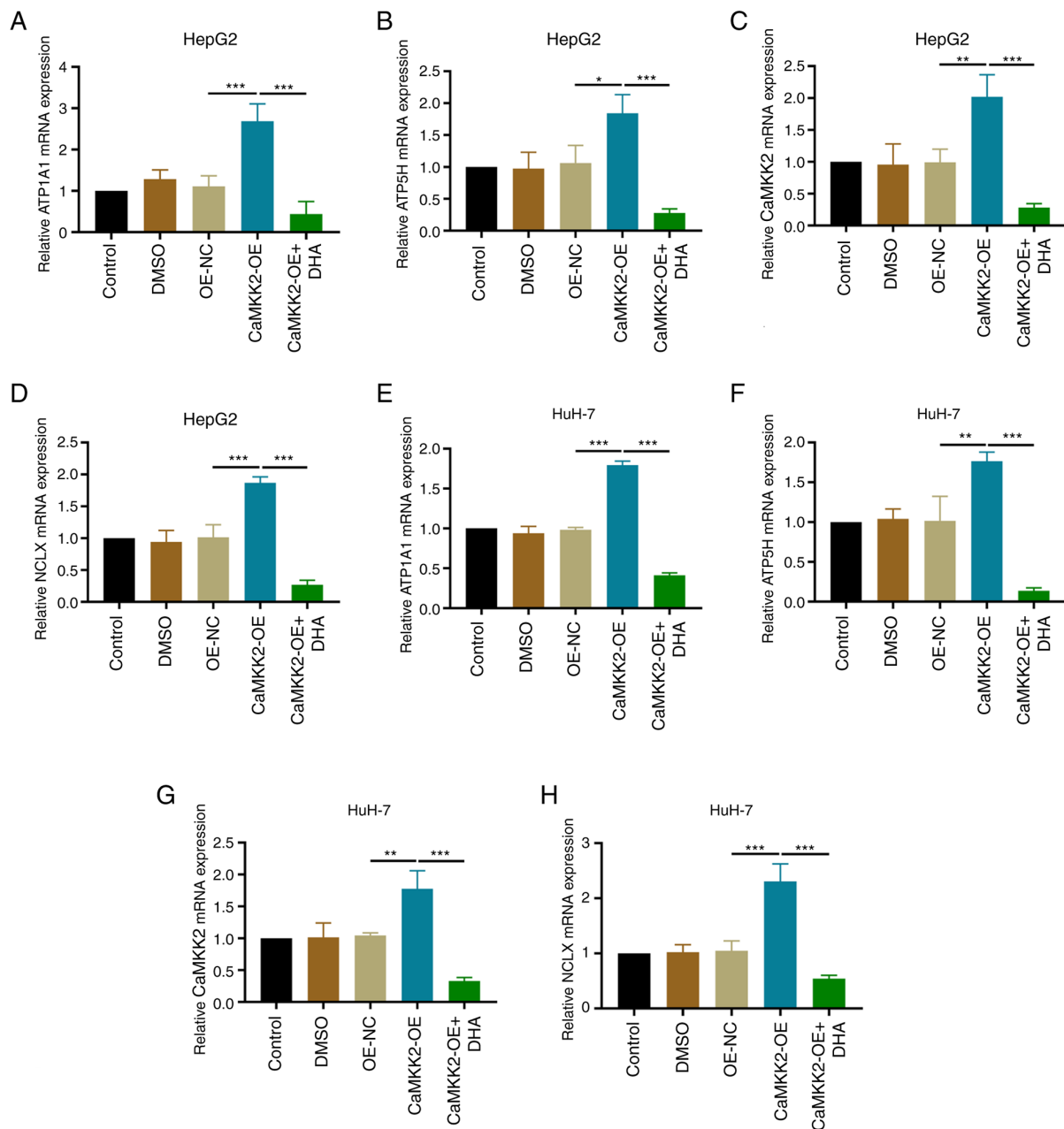


Figure 7. Effects of DHA treatment and CaMKK2-OE on ATP synthase expression. Relative mRNA expression levels of (A) ATP1A1, (B) ATP5H, (C) CaMKK2 and (D) NCLX in HepG2 cells transfected with CaMKK2-OE and treated with DHA were detected by RT-qPCR. Relative mRNA expression levels of (E) ATP1A1, (F) ATP5H, (G) CaMKK2 and (H) NCLX in HuH-7 cells transfected with CaMKK2-OE and treated with DHA were detected by RT-qPCR. All data are presented as the mean  $\pm$  standard deviation (n=3). Data were analyzed using one-way analysis of variance followed by Bonferroni post hoc test. \*P<0.05; \*\*P<0.01; \*\*\*P<0.001. NCLX, mitochondrial sodium/calcium exchanger protein; DHA, dihydroartemisinin; CaMKK2, calcium/calmodulin-dependent protein kinase kinase 2; OE, overexpression; RT-qPCR, reverse transcription-quantitative PCR; NC, negative control; ATP1A1, sodium/potassium-transporting ATPase subunit  $\alpha$ -1; ATP5H, ATP synthase subunit d, mitochondrial.

In addition, DHA can induce cell cycle arrest of liver cancer cells at the G<sub>0</sub>/G<sub>1</sub> phase, ROS generation and mitochondrial membrane potential loss, thereby leading to apoptosis (49). The present study demonstrated that CaMKK2-OE can significantly upregulate ATP formation and promote ROS generation in liver cancer cells, whereas knocking down NCLX expression could block these regulatory effects of CaMKK2.

The concentration of ROS in tumor cells is typically 100X higher than that of healthy cells (50). It has been previously suggested that increasing ROS levels may hinder tumor growth by inducing cell cycle arrest (51). ROS and ROS-dependent

lipid peroxidation products (including prostaglandins and active aldehydes) activate apoptosis through mitochondrial or endoplasmic reticulum stress-dependent pathways (52). By contrast, it has also been reported that ROS, as a signal molecule that induces the proliferation of cancer cells, is involved in the tumorigenic phenotype of cancer cells. ROS can activate EGFR, leading to the activation of the Ras/MAPK pathway involved in cell proliferation (53). In the present study, CaMKK2-OE promoted ROS increase, while DHA treatment significantly inhibited ROS production, thereby exhibiting antitumor activity. In summary, there are different views on the

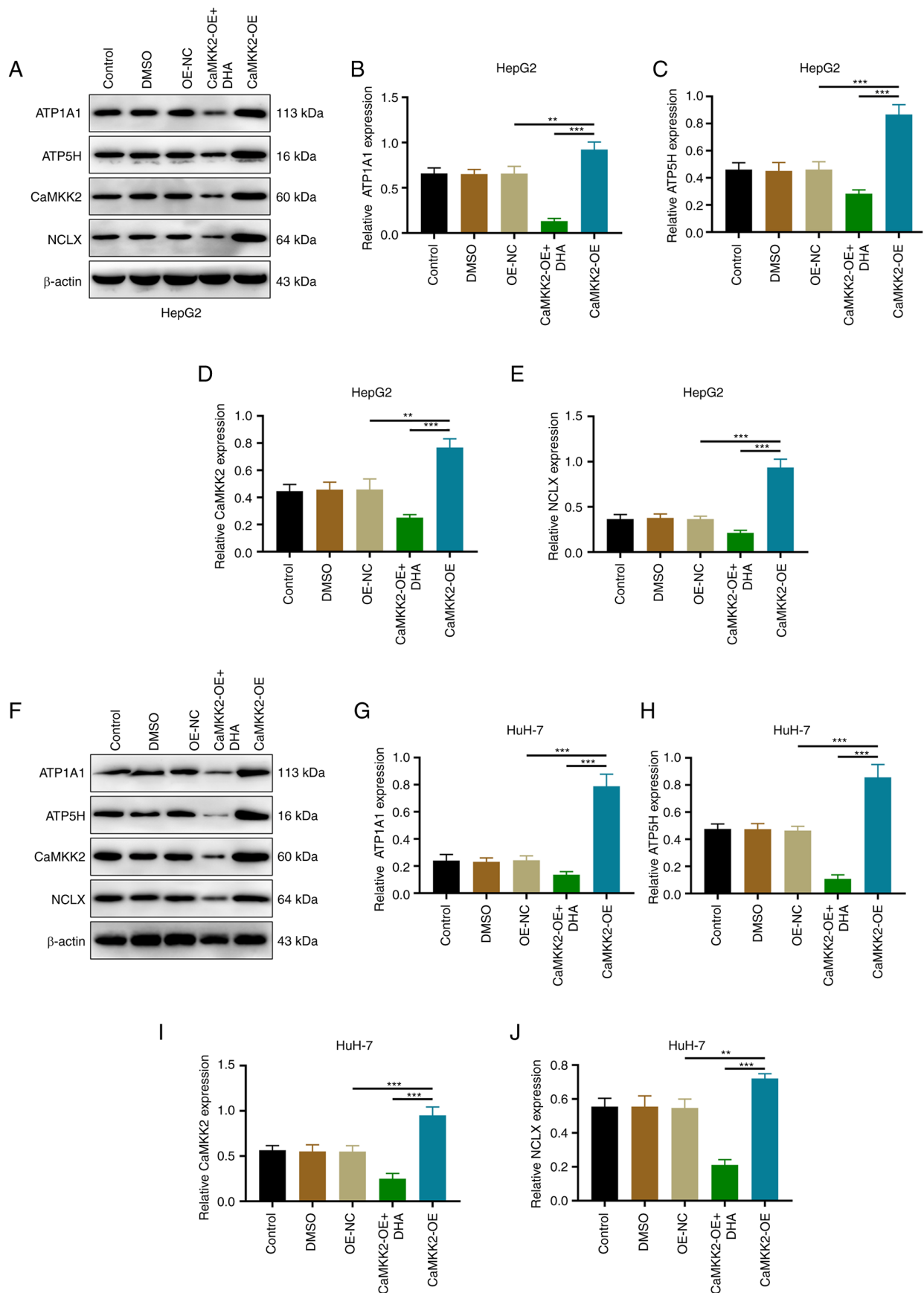


Figure 8. Effects of DHA treatment and CaMKK2-OE on ATP synthase expression. (A) Western blotting and protein expression levels of (B) ATP1A1, (C) ATP5H, (D) CaMKK2 and (E) NCLX in HepG2 cells transfected with CaMKK2-OE and treated with DHA. (F) Western blotting and protein expression levels of (G) ATP1A1, (H) ATP5H, (I) CaMKK2 and (J) NCLX in HuH-7 cells transfected with CaMKK2-OE and treated with DHA. All data are presented as the mean  $\pm$  standard deviation (n=3). Data were analyzed using one-way analysis of variance followed by Bonferroni post hoc test. \*\*P<0.01; \*\*\*P<0.001. NCLX, mitochondrial sodium/calcium exchanger protein; DHA, dihydroartemisinin; CaMKK2, calcium/calmodulin-dependent protein kinase kinase 2; OE, overexpression; NC, negative control; ATP1A1, sodium/potassium-transporting ATPase subunit  $\alpha$ -1; ATP5H, ATP synthase subunit d, mitochondrial.

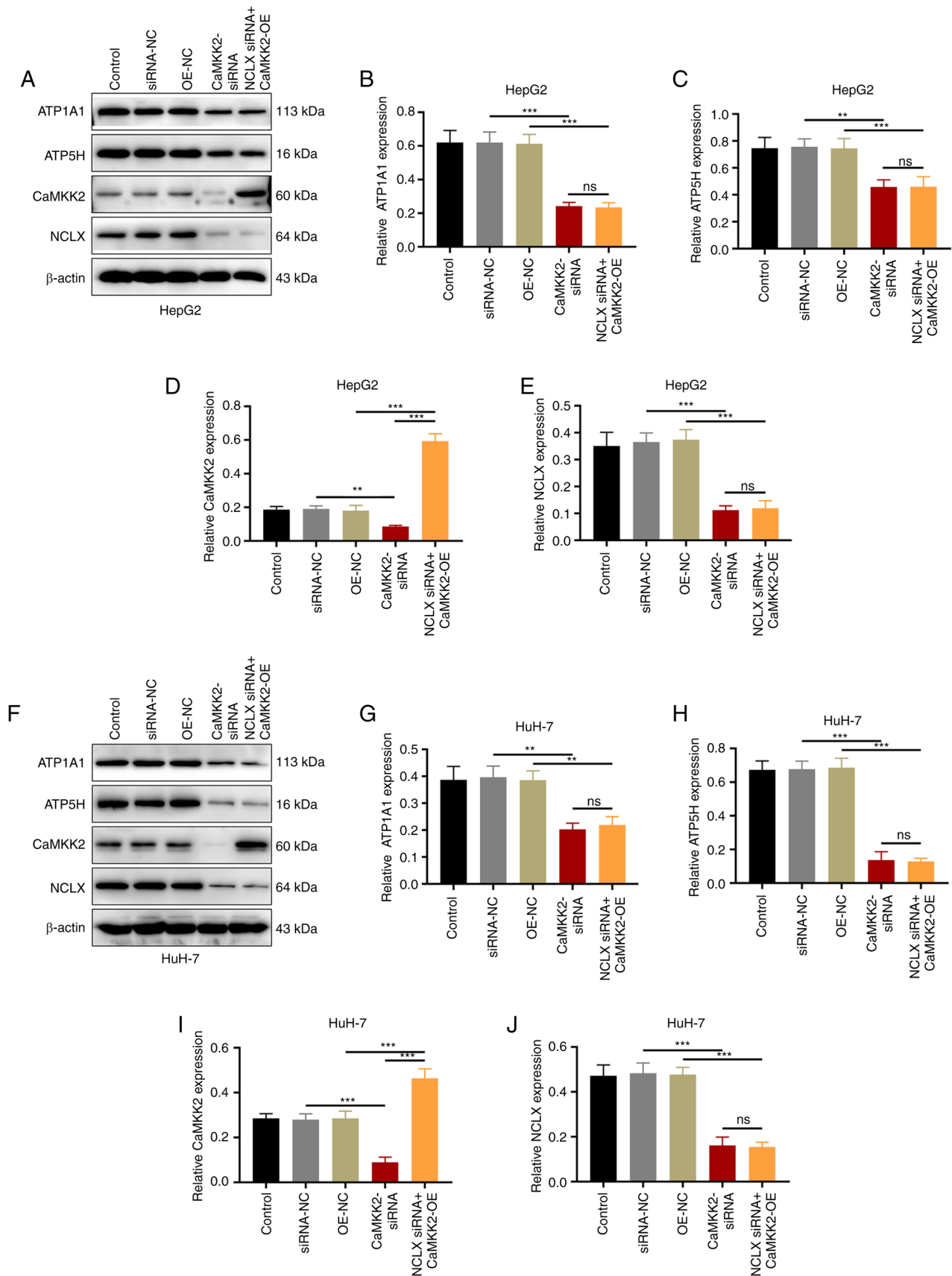


Figure 9. Effects of DHA treatment, CaMKK2 siRNA, CaMKK2-OE and NCLX siRNA on ATP synthase expression. (A) Western blotting and protein expression levels of (B) ATP1A1, (C) ATP5H, (D) CaMKK2 and (E) NCLX in HepG2 cells transfected with CaMKK2 siRNA, CaMKK2-OE and NCLX siRNA and treated with DHA. (F) Western blotting and protein expression levels of (G) ATP1A1, (H) ATP5H, (I) CaMKK2 and (J) NCLX in HuH-7 cells transfected with CaMKK2 siRNA, CaMKK2-OE and NCLX siRNA and treated with DHA. All data are presented as the mean  $\pm$  standard deviation (n=3). Data were analyzed using one-way analysis of variance followed by Bonferroni post hoc test. \*\*P<0.01, \*\*\*P<0.001. NCLX, mitochondrial sodium/calcium exchanger protein; DHA, dihydroartemisinin; CaMKK2, calcium/calmodulin-dependent protein kinase kinase 2; siRNA, small interfering RNA; OE, overexpression; ns, not significant; NC, negative control; ATP1A1, sodium/potassium-transporting ATPase subunit  $\alpha$ -1; ATP5H, ATP synthase subunit d, mitochondrial.

role of ROS in cancer progression, possibly because it changes at different stages of disease development. It is undeniable that ROS may be one of the monitoring indicators during cancer treatment.

Among mitochondrial calcium regulatory proteins, NCLX exerts a precancerous effect by regulating sodium-calcium exchange (54). Upregulating NCLX facilitates the release of mitochondrial  $\text{Ca}^{2+}$  and enhances cisplatin resistance in cancer cells (55). It has been found that epinephrine can stimulate NCLX-null BAT-induced  $\text{Ca}^{2+}$  overload, trigger the opening of mitochondrial permeability transition pore (mPTP), resulting in significant mitochondrial swelling and cell death (56). Furthermore, increasing NCLX levels can protect sensory neurons from cell damage caused by neurite degeneration and calcium accumulation (57). In the present study, knocking down NCLX significantly inhibited the proliferation, migration and invasion of liver cancer cells while reducing ATP and ROS production. The results of the present study showed that NCLX plays a key role in the proliferation, metastasis and mitochondrial function of liver cancer cells, which may be related to the regulation of calcium ions or may be affected by calcium regulation-related proteins. Knockout of NCLX inhibited the induction of ATP and ROS by CaMKK2-OE in cancer cells. It is worth noting that it did not affect the expression level of CaMKK2, similarly to the effect of NCLX siRNA alone. However, there was no significant difference between NCLX siRNA alone and NCLX siRNA + CaMKK2 OE group, indicating that NCLX had no effect on the expression of CaMKK2 in the process of blocking the regulation of CaMKK2, which further proved that NCLX was likely to be a downstream regulator of CaMKK2. Of course, other factors or genes playing a role in this process cannot be ruled out. Notably, the present study also demonstrated a significant reduction in the expression levels of CaMKK2 and NCLX with DHA treatment. In addition, DHA reduced the formation of ATP and ROS induced by CaMKK2-OE in cancer cells, further indicating that DHA inhibited the invasion and migration of liver cancer cells through this effect. Therefore, DHA may serve a role in inhibiting the metastatic phenotype of liver cancer cells through the CaMKK2/NCLX signaling pathway. It cannot be ignored that under physiological conditions, mitochondrial  $\text{Ca}^{2+}$  maintains  $\text{Ca}^{2+}$  homeostasis and ATP production through mitochondrial  $\text{Ca}^{2+}$  uniporter and NCLX to avoid cell death caused by too little  $\text{Ca}^{2+}$  or  $\text{Ca}^{2+}$  overload (58).

The failure of liver cancer treatment is multifaceted, especially for highly invasive cells, which undoubtedly increases the difficulty of treatment due to their complex energy metabolism pathways. Therefore, finding natural compounds for key proteins in the energy metabolism pathway may be a boon for the treatment of cancer patients (59,60). It has been reported that natural products have a synergistic effect on cancer immunotherapy (cancer vaccines, immune checkpoint inhibitors and adoptive immunotherapy). In particular, saponins, polysaccharides and flavonoids can exert a strong anti-tumor immune effect by reversing the tumor immunosuppressive microenvironment and combining with cancer immunotherapy (61). For example, DHA has previously been reported to exert significant anticancer effects, as it was shown to induce apoptosis, reduce angiogenesis and decrease drug resistance of breast cancer

cells (MDA-MB-231 and MDA-MB-436) (62). The present study demonstrated that DHA inhibited the production of ATP synthase (ATP1A1 and ATP5H subunits) in liver cancer cells, which was upregulated through the CaMKK2/NCLX pathway. AMPK is dependent on CaMKK2 (63) and the results of the present study showed that CaMKK2 can also mediate the anti-cancer effect of DHA through the NCLX pathway, enriching the CaMKK2 signal and can also act through the NCLX pathway mediating the anticancer effect of DHA. Tumor mitochondria are directly involved in the formation of the immune microenvironment (64). Tumor cell mitochondria inhibit or stimulate tumor growth and migration by releasing mitochondrial DNA, ATP, cytochrome *c* or formyl peptide to the extracellular matrix, thereby activating immune cells, which leads to proinflammatory and immunosuppressive reactions (65). DHA may affect the immune microenvironment by regulating mitochondrial function, which may also improve the therapeutic effect of immunosuppressive agents. Further studies are required in the future to investigate this hypothesis. Mutations in mitochondrial calcium-related proteins have different effects on the cytoskeleton (for instance, GDAP1 loss of function inhibits the mitochondrial pyruvate dehydrogenase complex by altering the actin cytoskeleton). By observing changes in the fluorescence intensity of microfilaments, which reflect their stability, it was demonstrated that different stress response patterns of liver cancer cells could be induced by CaMKK2-OE, knockdown of NCLX or DHA treatment. This has potential implications for elucidating the molecular mechanisms by which DHA targets mitochondrial calcium regulatory proteins to inhibit liver cancer metastasis.

In conclusion, the present study demonstrated that DHA may inhibit liver cancer cell proliferation, ROS production and metastatic phenotype by reducing ATP synthase production through the CaMKK2/NCLX signaling pathway. The present study highlighted a potential future treatment for liver cancer using a natural drug derivative, which targeted calcium homeostasis to disrupt the metabolism of cancer cells. It is essential to further explore the effectiveness of DHA as an anticancer drug to enhance its utility in the treatment of liver cancer.

## Acknowledgements

Not applicable.

## Funding

This work was supported by the High Level Talents Project of Hainan Natural Science Foundation of 2022 (grant no. 822RC830) and the Hainan Health Industry Scientific Research Project of 2021 (grant no. 21A200072).

## Availability of data and materials

The datasets used and/or analyzed during the current study are available from the corresponding author on reasonable request.

## Authors' contributions

JC and CX designed the experiments. CX and YiW performed the experiments and collected data. YoW, CX and JC discussed



the results and strategy. YoW analyzed and interpreted the data, YiW and JC supervised, directed and managed the study. JC and YoW confirm the authenticity of all the raw data. All authors read and approved the final version of the manuscript.

#### Ethics approval and consent to participate

Not applicable.

#### Patient consent for publication

Not applicable.

#### Competing interests

The authors declare that they have no competing interests.

#### References

- Stewart LM, Gerner L, Rettel M, Stein F, Burrows JF, Mills IG and Evergren E: CaMKK2 facilitates Golgi-associated vesicle trafficking to sustain cancer cell proliferation. *Cell Death Dis* 12: 1040, 2021.
- Raturi A, Gutiérrez T, Ortiz-Sandoval C, Ruangkittisakul A, Herrera-Cruz MS, Rockley JP, Gesson K, Ourdev D, Lou PH, Lucchinetti E, *et al*: TMX1 determines cancer cell metabolism as a thiol-based modulator of ER-mitochondria Ca<sup>2+</sup> flux. *J Cell Biol* 214: 433-444, 2016.
- Williams JN and Sankar U: CaMKK2 signaling in metabolism and skeletal disease: A new axis with therapeutic potential. *Curr Osteoporos Rep* 17: 169-177, 2019.
- Pulliam TL, Goli P, Awad D, Lin C, Wilkenfeld SR and Frigo DE: Regulation and role of CAMKK2 in prostate cancer. *Nat Rev Urol* 19: 367-380, 2022.
- Han JH, Kim YK, Kim H, Lee J, Oh MJ, Kim SB, Kim M, Kim KH, Yoon HJ, Lee MS, *et al*: Snail acetylation by autophagy-derived acetyl-coenzyme A promotes invasion and metastasis of KRAS-LKB1 co-mutated lung cancer cells. *Cancer Commun (Lond)* 42: 716-749, 2022.
- Lin F, Marcelo KL, Rajapakse K, Coarfa C, Dean A, Wilganowski N, Robinson H, Sevcik E, Bissig KD, Goldie LC, *et al*: The camKK2/camKIV relay is an essential regulator of hepatic cancer. *Hepatology* 62: 505-520, 2015.
- Dai S, Venturini E, Yadav S, Lin X, Clapp D, Steckiewicz M, Gocher-Demske AM, Hardie DG and Edelman AM: Calcium/calmodulin-dependent protein kinase kinase 2 mediates pleiotropic effects of epidermal growth factor in cancer cells. *Biochim Biophys Acta Mol Cell Res* 1869: 119252, 2022.
- Pathak T, Gueguinou M, Walter V, Delierneux C, Johnson MT, Zhang X, Xin P, Yeast RE, Emrich SM, Yochum GS, *et al*: Dichotomous role of the human mitochondrial Na<sup>+</sup>/Ca<sup>2+</sup>/Li<sup>+</sup> exchanger NCLX in colorectal cancer growth and metastasis. *eLife* 9: e59686, 2020.
- Guéguinou M, Ibrahim S, Bourgeois J, Robert A, Pathak T, Zhang X, Crottès D, Dupuy J, Ternant D, Monbet V, *et al*: Curcumin and NCLX inhibitors share anti-tumoral mechanisms in microsatellite-instability-driven colorectal cancer. *Cell Mol Life Sci* 79: 284, 2022.
- Ruiz A, Alberdi E and Matute C: CGP37157, an inhibitor of the mitochondrial Na<sup>+</sup>/Ca<sup>2+</sup> exchanger, protects neurons from excitotoxicity by blocking voltage-gated Ca<sup>2+</sup> channels. *Cell Death Dis* 5: e1156, 2014.
- Ni Z, He J, Wu Y, Hu C, Dai X, Yan X, Li B, Li X, Xiong H, Li Y, *et al*: AKT-mediated phosphorylation of ATG4B impairs mitochondrial activity and enhances the Warburg effect in hepatocellular carcinoma cells. *Autophagy* 14: 685-701, 2018.
- Ge Q, Jia D, Cen D, Qi Y, Shi C, Li J, Sang L, Yang L, He J, Lin A, *et al*: Micropeptide ASAP encoded by LINC00467 promotes colorectal cancer progression by directly modulating ATP synthase activity. *J Clin Invest* 131: e152911, 2021.
- Jiang W, Wang L, Zhang Y and Li H: Circ-ATP5H Induces Hepatitis B Virus replication and expression by regulating miR-138-5p/TNFAIP3 axis. *Cancer Manag Res* 12: 11031-11040, 2020.
- Feng XY, Zhao W, Yao Z, Wei NY, Shi AH and Chen WH: Downregulation of ATP1A1 Expression by Panax notoginseng (Burk.) F.H. Chen Saponins: A potential mechanism of antitumor effects in HepG2 cells and in vivo. *Front Pharmacol* 12: 720368, 2021.
- Althurwi SI, Yu JQ, Beale P and Huq F: Sequenced combinations of cisplatin and selected phytochemicals towards overcoming drug resistance in ovarian tumour models. *Int J Mol Sci* 21: 7500, 2020.
- Xu T, Yang Y, Chen Z, Wang J, Wang X, Zheng Y, Wang C, Wang Y, Zhu Z, Ding X, *et al*: TNFAIP2 confers cisplatin resistance in head and neck squamous cell carcinoma via KEAP1/NRF2 signaling. *J Exp Clin Cancer Res* 42: 190, 2023.
- Song KH, Kim JH, Lee YH, Bae HC, Lee HJ, Woo SR, Oh SJ, Lee KM, Yee C, Kim BW, *et al*: Mitochondrial reprogramming via ATP5H loss promotes multimodal cancer therapy resistance. *J Clin Invest* 128: 4098-4114, 2018.
- Huang CJ, Zhang CY, Zhao YK, Wang D, Zhuang L, Qian L, Xie L, Zhu Y and Meng ZQ: Bufalin inhibits tumorigenesis and SREBP-1-mediated lipogenesis in hepatocellular carcinoma via modulating the ATP1A1/CA2 axis. *Am J Chin Med* 51: 461-485, 2023.
- Zhou W, Chen MM, Liu HL, Si ZL, Wu WH, Jiang H, Wang LX, Vaziri ND, An XF, Su K, *et al*: Dihydroartemisinin suppresses renal fibrosis in mice by inhibiting DNA-methyltransferase 1 and increasing Klotho. *Acta Pharmacol Sin* 43: 2609-2623, 2022.
- Chen YI, Chang CC, Hsu MF, Jeng YM, Tien YW, Chang MC, Chang YT, Hu CM and Lee WH: Homophilic ATP1A1 binding induces activin A secretion to promote EMT of tumor cells and myofibroblast activation. *Nat Commun* 13: 2945, 2022.
- Eskiocak U, Ramesh V, Gill JG, Zhao Z, Yuan SW, Wang M, Vandergriff T, Shackleton M, Quintana E, Johnson TM, *et al*: Synergistic effects of ion transporter and MAP kinase pathway inhibitors in melanoma. *Nat Commun* 7: 12336, 2016.
- Peng J, Wang Q, Zhou J, Zhao S, Di P, Chen Y, Tao L, Du Q, Shen X and Chen Y: Targeted lipid nanoparticles encapsulating dihydroartemisinin and chloroquine phosphate for suppressing the proliferation and liver metastasis of colorectal cancer. *Front Pharmacol* 12: 720777, 2021.
- Shi H, Xiong L, Yan G, Du S, Liu J and Shi Y: Susceptibility of cervical cancer to dihydroartemisinin-induced ferritinophagy-dependent ferroptosis. *Front Mol Biosci* 10: 1156062, 2023.
- Zhang J, Li Y, Wang JG, Feng JY, Huang GD and Luo CG: Dihydroartemisinin affects STAT3/DDA1 signaling pathway and reverses breast cancer resistance to cisplatin. *Am J Chin Med* 51: 445-459, 2023.
- Wu S, Li Z, Li H and Liao K: Dihydroartemisinin reduces irradiation-induced mitophagy and radioresistance in lung cancer A549 cells via CIRBP Inhibition. *Life (Basel)* 12: 1129, 2022.
- Chen X, Cui Y and Ma Y: Long non-coding RNA BLACAT1 expedites osteosarcoma cell proliferation, migration and invasion via up-regulating SOX12 through miR-608. *J Bone Oncol* 25: 100314, 2020.
- Wang X, Zheng D, Wang C and Chen W: Knockdown of circ\_0005615 enhances the radiosensitivity of colorectal cancer by regulating the miR-665/NOTCH1 axis. *Open Med (Wars)* 18: 20230678, 2023.
- Livak K and Schmittgen T: Analysis of relative gene expression data using real-time quantitative PCR and the 2<sup>-ΔΔC<sub>T</sub></sup> method. *Methods* 25: 402-408, 2001.
- Liu Y, Wang R, Huang R, Rutz B, Ciotkowska A, Tamalunas A, Hu S, Trieb M, Waidelich R, Strittmatter F, *et al*: Inhibition of growth and contraction in human prostate stromal cells by silencing of NUA1 and -2, and by the presumed NUA1 inhibitors HTH01-015 and WZ4003. *Front Pharmacol* 14: 1105427, 2023.
- Zheng Y, Liu P, Wang N, Wang S, Yang B, Li M, Chen J, Situ H, Xie M, Lin Y, *et al*: Betulinic acid suppresses breast cancer metastasis by targeting GRP78-mediated glycolysis and ER stress apoptotic pathway. *Oxid Med Cell Longev* 2019: 8781690, 2019.
- Pavlova NN, Zhu J and Thompson CB: The hallmarks of cancer metabolism: Still emerging. *Cell Metab* 34: 355-377, 2022.
- Bonora M, Patergnani S, Rimessi A, De Marchi E, Suski JM, Bononi A, Giorgi C, Marchi S, Missiroli S, Poletti F, *et al*: ATP synthesis and storage. *Purinergic Signal* 8: 343-357, 2012.
- Brookes PS, Yoon Y, Robotham JL, Anders MW and Sheu SS: Calcium, ATP and ROS: A mitochondrial love-hate triangle. *Am J Physiol Cell Physiol* 287: C817-C833, 2004.

34. Ponneri Babu Harisankar A, Kuo CL, Chou HY, Tangeda V, Fan CC, Chen CH, Kao YH and Lee AY: Mitochondrial Lon-induced mitophagy benefits hypoxic resistance via  $\text{Ca}^{2+}$ -dependent FUNDC1 phosphorylation at the ER-mitochondria interface. *Cell Death Dis* 14: 199, 2023.
35. Wells C, Liang Y, Pulliam TL, Lin C, Awad D, Eduful B, O'Byrne S, Hossain MA, Catta-Preta CMC, Ramos PZ, *et al.*: SGC-CAMKK2-1: A chemical probe for CAMKK2. *Cells* 12: 287, 2023.
36. Wang X, Cheng G, Miao Y, Qiu F, Bai L, Gao Z, Huang Y, Dong L, Niu X, Wang X, *et al.*: Piezo type mechanosensitive ion channel component 1 facilitates gastric cancer omentum metastasis. *J Cell Mol Med* 25: 2238-2253, 2021.
37. Sarkar A, Novohradsky V, Maji M, Babu T, Markova L, Kostrehunova H, Kasparkova J, Gandin V, Brabec V and Gibson D: Multitargeting prodrugs that release oxaliplatin, doxorubicin and gemcitabine are potent inhibitors of tumor growth and effective inducers of immunogenic cell death. *Angew Chem Int Ed Engl* 62: e202310774, 2023.
38. Singh J, Meena A and Luqman S: New frontiers in the design and discovery of therapeutics that target calcium ion signaling: A novel approach in the fight against cancer. *Expert Opin Drug Discov* 1: 1-14, 2023.
39. Que Z, Zhou Z, Liu S, Zheng W and Lei B: Dihydroartemisinin inhibits EMT of glioma via gene BASP1 in extrachromosomal DNA. *Biochem Biophys Res Commun* 675: 130-138, 2023.
40. Fan M, Zhang J, Tsai CW, Orlando BJ, Rodriguez M, Xu Y, Liao M, Tsai MF and Feng L: Structure and mechanism of the mitochondrial  $\text{Ca}^{2+}$  uniporter holocomplex. *Nature* 582: 129-133, 2020.
41. Kennedy G, Gibson O, O'Hare D, Mills IG and Evergren E: The role of CaMKK2 in Golgi-associated vesicle trafficking. *Biochem Soc Trans* 51: 331-342, 2023.
42. Stork BA, Dean A, Ortiz AR, Saha P, Putluri N, Planas-Silva MD, Mahmud I, Rajapakshe K, Coarfa C, Knapp S, *et al.*: Calcium/calmodulin-dependent protein kinase kinase 2 regulates hepatic fuel metabolism. *Mol Metab* 62: 101513, 2022.
43. Najar M, Arefian M, Sidransky D, Gowda H, Prasad T, Modi P and Chatterjee A: Tyrosine phosphorylation profiling revealed the signaling network characteristics of CAMKK2 in gastric adenocarcinoma. *Front Genet* 13: 854764, 2022.
44. Najar MA, Aravind A, Dagamajalu S, Sidransky D, Ashktorab H, Smoot DT, Gowda H, Prasad TSK, Modi PK and Chatterjee A: Hyperactivation of MEK/ERK pathway by  $\text{Ca}^{2+}$ /calmodulin-dependent protein kinase kinase 2 promotes cellular proliferation by activating cyclin-dependent kinases and minichromosome maintenance protein in gastric cancer cells. *Mol Carcinog* 60: 769-783, 2021.
45. Waseem M and Wang BD: Promising strategy of mPTP modulation in cancer therapy: An emerging progress and future insight. *Int J Mol Sci* 24: 5564, 2023.
46. Su Y, Zhao D, Jin C, Li Z, Sun S, Xia S, Zhang Y, Zhang Z, Zhang F, Xu X, *et al.*: Dihydroartemisinin induces ferroptosis in HCC by promoting the formation of PEBP1/15-LO. *Oxid Med Cell Longev* 2021: 3456725, 2021.
47. Fu F, Wang W, Wu L, Wang W, Huang Z, Huang Y, Wu C and Pan X: Inhalable Biomimetic liposomes for cyclic  $\text{Ca}^{2+}$ -Burst-centered endoplasmic reticulum stress enhanced lung cancer ferroptosis therapy. *ACS Nano* 17: 5486-5502, 2023.
48. Timm KN, Hu DE, Williams M, Wright AJ, Kettunen MI, Kennedy BWC, Larkin TJ, Dzien P, Marco-Rius I, Bohndiek SE, *et al.*: Assessing oxidative stress in tumors by measuring the rate of hyperpolarized [1- $^{13}\text{C}$ ]Dehydroascorbic acid reduction using  $^{13}\text{C}$  magnetic resonance spectroscopy. *J Biol Chem* 292: 1737-1748, 2017.
49. Hsu YF, Kung FL, Huang TE, Deng YN, Guh JH, Marchetti P, Marchesi E, Perrone D, Navacchia ML and Hsu LC: Anticancer activity and molecular mechanisms of an ursodeoxycholic acid methyl Ester-dihydroartemisinin hybrid via a triazole linkage in hepatocellular carcinoma Cells. *Molecules* 28: 2358, 2023.
50. Szatrowski TP and Nathan CF: Production of large amounts of hydrogen peroxide by human tumor cells. *Cancer Res* 51: 794-798, 1991.
51. Jia F, Liu Y, Dou X, Du C, Mao T and Liu X: Liensinine inhibits osteosarcoma growth by ROS-mediated suppression of the JAK2/STAT3 signaling pathway. *Oxid Med Cell Longev* 2022: 8245614, 2022.
52. Wójcik P, Żarković N, Gęgotek A and Skrzydlewska E: Involvement of metabolic lipid mediators in the regulation of apoptosis. *Biomolecules* 10: 402, 2020.
53. Han H, Lim JW and Kim H: Lycopene inhibits activation of epidermal growth factor receptor and expression of cyclooxygenase-2 in gastric cancer cells. *Nutrients* 11: 2113, 2019.
54. Katoshevski T, Bar L, Tikochinsky E, Harel S, Ben-Kasus Nissim T, Bogeski I, Hershfinkel M, Attali B and Sekler I: CKII control of axonal plasticity is mediated by mitochondrial  $\text{Ca}^{2+}$  via mitochondrial NCLX. *Cells* 11: 3990, 2022.
55. Tangeda V, Lo YK, Babu Harisankar AP, Chou HY, Kuo CL, Kao YH, Lee AY and Chang JY: Lon upregulation contributes to cisplatin resistance by triggering NCLX-mediated mitochondrial  $\text{Ca}^{2+}$  release in cancer cells. *Cell Death Dis* 13: 241, 2022.
56. Assali EA, Jones AE, Veliova M, Acín-Pérez R, Taha M, Miller N, Shum M, Oliveira MF, Las G, Liesa M, *et al.*: NCLX prevents cell death during adrenergic activation of the brown adipose tissue. *Nat Commun* 11: 3347, 2020.
57. Britti E, Delaspre F, Tamarit J and Ros J: Calpain-inhibitors protect frataxin-deficient dorsal root ganglia neurons from loss of mitochondrial  $\text{Na}^{+}/\text{Ca}^{2+}$  exchanger, NCLX, and apoptosis. *Neurochem Res* 46: 108-119, 2021.
58. Lee SH, Duron HE and Chaudhuri D: Beyond the TCA cycle: New insights into mitochondrial calcium regulation of oxidative phosphorylation. *Biochem Soc Trans* 51: 1661-1673, 2023.
59. Zhao H, Yan G, Zheng L, Zhou Y, Sheng H, Wu L, Zhang Q, Lei J, Zhang J, Xin R, *et al.*: STIM1 is a metabolic checkpoint regulating the invasion and metastasis of hepatocellular carcinoma. *Theranostics* 10: 6483-6499, 2020.
60. Liu M, Jin L, Sun S, Liu P, Feng X, Cheng Z, Liu W, Guan K, Shi Y, Yuan H, *et al.*: Metabolic reprogramming by PCK1 promotes TCA cataplerosis, oxidative stress and apoptosis in liver cancer cells and suppresses hepatocellular carcinoma. *Oncogene* 37: 1637-1653, 2018.
61. Dong S, Guo X, Han F, He Z and Wang Y: Emerging role of natural products in cancer immunotherapy. *Acta Pharm Sin B* 12: 1163-1185, 2022.
62. Augimeri G, Fiorillo M, Morelli C, Panza S, Giordano C, Barone I, Catalano S, Sisci D, Andò S and Bonfiglioglio D: The Omega-3 docosahexaenoyl ethanolamide reduces CCL5 secretion in triple negative breast cancer cells affecting tumor progression and macrophage recruitment. *Cancers (Basel)* 15: 819, 2023.
63. Tompkins E, Mimic B, Penn RB and Pera T: The biased M3 mAChR ligand PD 102807 mediates qualitatively distinct signaling to regulate airway smooth muscle phenotype. *J Biol Chem* 299: 105209, 2023.
64. Du F, Yang L, Liu J, Wang J, Fan L, Duangmano S, Liu H, Liu M, Wang J, Zhong X, *et al.*: The role of mitochondria in the resistance of melanoma to PD-1 inhibitors. *J Transl Med* 21: 345, 2023.
65. Sahinbegovic H, Jelinek T, Hrdinka M, Bago JR, Turi M, Sevcikova T, Kurtovic-Kozaric A, Hajek R and Simicek M: Intercellular mitochondrial transfer in the tumor microenvironment. *Cancers (Basel)* 12: 1787, 2020.



Copyright © 2023 Chang *et al.* This work is licensed under a Creative Commons Attribution-NonCommercial-NoDerivatives 4.0 International (CC BY-NC-ND 4.0) License.